Energy-band structure of Ge, Si, and GaAs: A thirty-band k·p method

Soline Richard, Frédéric Aniel, and Guy Fishman
Institut d'Électronique Fondamentale, UMR 8622 CNRS, Université Paris Sud, 91405 Orsay Cedex, France
(Received 3 February 2004; published 3 December 2004)

A 30-band **k·p** method taking into account spin-orbit coupling is used to describe the band diagram of Ge, Si, and GaAs over the whole Brillouin zone on an extent of 5 eV above and 6 eV under the top of the valence band. The band diagrams provide effective masses in agreement with experimental data both for direct gap semiconductors (GaAs) and for indirect gap semiconductors (Ge, Si). This method also gives explicit expressions for Luttinger parameters and effective masses in the Γ valley.

DOI: 10.1103/PhysRevB.70.235204 PACS number(s): 71.15.Ap, 71.20.Mq

I. INTRODUCTION

Dispersion relations of bulk materials have been intensively studied through two sets of methods: the first set contains theories with few adjustable parameters such as pseudopotential[1] or linear muffin-tin-orbital methods.[2] In the best case, only one adjustable parameter, the forbidden band gap, is required.[1] The second set contains adjustable parameter theories namely the linear combination of atomic orbitals,[3] tight-binding,[4] and **k·p**[5] methods. The **k·p** method is known to be very efficient to accurately describe either the conduction band[6] or the valence band[7,8] or even both of them[9,10] in the vicinity of a given point of the Brillouin zone. For example, Pidgeon and Brown[10] used Luttinger-like parameters inside an eight-function basis (taking into account the spin) to describe the dispersion curves near the center of the Brillouin zone. The Luttinger-like parameters allow one to take into account the influence of the functions outside the eight-function basis. The Pidgeon-Brown description is valid up to about 15% of the Brillouin zone, the validity range depending on some parameters as the forbidden gap. Afterwards, a 14-function basis (with spin)[11] was used, the aim being a more accurate description of both the band structure and the eigen wave functions, more than an increase of the validity range. Cardona and Pollak[5] used the **k·p** method with another point of view: they used a 15-function basis (without spin) to describe the dispersion curve in the whole Brillouin zone. They reproduced the band structure of silicon and germanium without taking the influence of function outside the 15-function basis: Luttinger-like parameters are not needed anymore and, in this sense, the Cardona-Pollak basis is self-contained. This 15-band method leads to a 30-band method if the spin is taken into account, which seems hardly tractable. This is the reason why Cavassilas *et al.*[12] used a 20-function basis (with spin) and introduced two bands named *s** and pseudo-Luttinger parameters to mimic *d* levels following the idea developed by Vogl *et al.*[4] for linear combination of atomic orbitals (LCAO) calculations. With this 20-band **k·p** Hamiltonian model, valleys useful for transport (Γ, *L*, and *X* valleys in GaAs, Δ and *L* valleys in Si) were obtained but this model contained ten adjustable parameters to describe *s** bands, nine interaction energies between bands for T_d group semiconductors (only six for O_h group semiconductors) and six pseudo-Luttinger parameters, i.e., 25 adjustable parameters. Moreover, this 20-band Hamiltonian gave valid results up to 3.5 eV above the top of the valence band and did not give access to the *L* valley of the second conduction band.

The purpose of this paper is to present a 30-band **k·p** Hamiltonian which allows us to calculate the band diagram of bulk materials for T_d or O_h group semiconductors. This Hamiltonian looks like the one of Ref. 5 for Si and Ge: we have taken the same basis states but we have introduced spin-orbit interaction which cannot be neglected in Ge or GaAs in which the spin-orbit splitting is more than 20% of the band gap energy. Bailey *et al.*[13] have taken into account spin-orbit interaction in their band structure calculation in GaAs over the whole Brillouin zone. We will compare their results to ours before concluding. For Si, even if the spin-orbit splitting may be neglected ($\Delta_{so}=44$ meV$\ll E_G=1.17$ eV) to draw the band diagram, taking it into account gives access to explicit expressions of the Luttinger parameters. With this Hamiltonian, the band diagram becomes valid up to 5 eV above and 6 eV under the top of the valence band all over the Brillouin zone. In particular this procedure solves the problem of the *L* point of the second conduction band of the 20-band **k·p** approach. This paper is organized as follows. In Sec. II, we present the procedure followed to build the Hamiltonian, which is used in Sec. III to obtain Si, Ge, and GaAs band diagrams. We show in Sec. III that ten adjustable parameters in O_h group and 18 in T_d group (7 of which are taken null to simulate GaAs) are sufficient. It is the reason why the 30-band method is not only more accurate than the 20-band method used in Ref. 12 but *in fine* more simple to use. In Sec. IV, we discuss the results and the validity of our Hamiltonian and compare them to other methods including the 20-band **k·p** method.[12]

II. THE 30-BAND k·p HAMILTONIAN

We start from the 15×15 **k·p** Hamiltonian without spin-orbit interaction built by Cardona and Pollak.[5] The 15 states of the real crystal taken into account correspond to [000], $(2\pi/a)$[111] and $(2\pi/a)$[200] plane-wave states of free electrons in the "empty" germanium lattice. The large gap between $(2\pi/a)$[200] and $(2\pi/a)$[220] plane waves (more than 15 eV) suggests that these 15 states are enough to obtain a correct energy band diagram. Introducing spin-orbit coupling doubles the number of states to obtain the so-called 30×30 **k·p** Hamiltonian.

We consider the Schrödinger equation with spin-orbit coupling

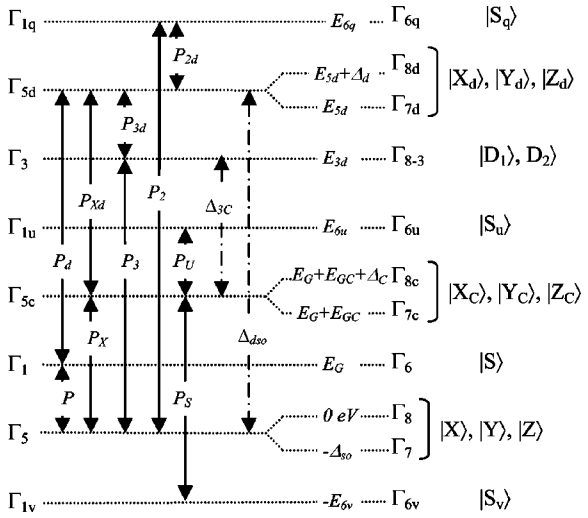

FIG. 1. Wave functions in the 30-band $\mathbf{k}\cdot\mathbf{p}$ model at $k=0$ for O_h group. T_d simple group notations are reported on the left, and T_d double group notations on the right. Only ten matrix elements are enough to describe the band diagram.

$$H\Psi = \left[\frac{\mathbf{p}^2}{2m_0} + V(\mathbf{r}) + \frac{\hbar}{4m_0^2c^2}(\nabla V \times \mathbf{p})\cdot\boldsymbol{\sigma}\right]\Psi = E\Psi, \quad (1)$$

where $V(\mathbf{r})$ is a potential having the periodicity of the lattice, m_0 is the free electron mass, $\mathbf{p}=-i\hbar\nabla$ and the spin-orbit term is written in standard notation. The solutions to Eq. (1) are Bloch functions $\Psi=\exp(i\mathbf{k}\cdot\mathbf{r})\,u_{n,k}(\mathbf{r})$, where $u_{n,k}(\mathbf{r})$ has the periodicity of the crystal lattice. The equation verified by the $u_{n,k}(\mathbf{r})$ is

$$H_{\mathrm{so}}u_{n,k}(\mathbf{r}) = \left[\frac{\mathbf{p}^2}{2m_0} + V(\mathbf{r}) + \frac{\hbar^2k^2}{2m_0} + \frac{\hbar}{m_0}\mathbf{k}\cdot\mathbf{p} + \frac{\hbar}{4m_0^2c^2}(\nabla V \times \mathbf{p})\cdot\boldsymbol{\sigma}\right]u_{n,k}(\mathbf{r}) = E_{n,k}u_{n,k}(\mathbf{r}). \quad (2)$$

The spin-orbit interaction term $(\hbar/4m_0^2c^2)(\nabla V\times\mathbf{k})\cdot\boldsymbol{\sigma}$ also exists but is negligible.[14] The states chosen by Cardona and Pollak[5] diagonalize the following Hamiltonian without the spin-orbit term

$$H_{kp}u_{n,k}(\mathbf{r}) = \left[\frac{\mathbf{p}^2}{2m_0} + V(\mathbf{r}) + \frac{\hbar^2k^2}{2m_0} + \frac{\hbar}{m_0}\mathbf{k}\cdot\mathbf{p}\right]u_{n,k}(\mathbf{r}) = E_{n,k}u_{n,k}(\mathbf{r}). \quad (3)$$

Let us first discuss the $\mathbf{k}\cdot\mathbf{p}$ terms associated with the Hamiltonian (2). This model, schematically represented at $k=0$ in Fig. 1, corresponds to the one used in Ref. 5; the correspondence between the level notations used in Ref. 5 and in this article is recalled in Table I and the wave functions associated to these levels are indicated in Fig. 1. For O_h group semiconductors (Si and Ge), the ten $\mathbf{k}\cdot\mathbf{p}$ matrix elements of interest are: $P=\langle S|p_x|iX\rangle$, $P_d=\langle S|p_x|iX_d\rangle$, $P_X=\langle X_C|p_y|iZ\rangle$, $P_{Xd}=\langle X_C|p_y|iZ_d\rangle$, $P_3=\langle D_1|p_x|iX\rangle$, $P_{3d}=\langle D_1|p_x|iX_d\rangle$, $P_2=\langle S_2|p_x|iX\rangle$, $P_{2d}=\langle S_2|p_x|iX_d\rangle$, $P_S=\langle S_v|p_x|iX_C\rangle$, $P_U=\langle S_U|p_x|iX_C\rangle$. Figure 2 represents the additional $\mathbf{k}\cdot\mathbf{p}$ matrix elements which have to be taken into account for the T_d group, because there is no inversion symmetry. These are matrix elements: $P'=\langle S|p_x|iX_C\rangle$, $P'_d=\langle X_d|p_y|iZ\rangle$, $P'_3=\langle D_1|p_x|iX_C\rangle$, $P'_2=\langle S_2|p_x|iX_C\rangle$, $P'_S=\langle S_v|p_x|iX\rangle$, $P'_{Sd}=\langle S_v|p_x|iX_d\rangle$, $P'_U=\langle S_U|p_x|iX\rangle$, $P'_{Ud}=\langle S_U|p_x|iX_d\rangle$.

TABLE I. Correspondence between Cardona and Pollak (Ref. 5) and Koster (Ref. 15) energy level notations for simple and double group. T_d group notations are used in the paper even for Si and Ge.

Simple group			Double group	
Ref. 5	O_h	T_d	O_h	T_d
$\Gamma^u_{2'}$	Γ^-_{2u}	Γ_{1q}	Γ^-_{7q}	Γ_{6q}
$\Gamma^u_{25'}$	Γ^+_{5d}	Γ_{5d}	$\Gamma^+_{8d}/\Gamma^+_{7d}$	Γ_{8d}/Γ_{7d}
Γ_{12},	Γ^-_3	Γ_3	Γ^-_{8d}	Γ_{8-3}
Γ^u_1	Γ^+_{1u}	Γ_{1u}	Γ^+_{6u}	Γ_{6u}
Γ_{15}	Γ^-_4	Γ_{5C}	Γ^-_8/Γ^-_6	Γ_{8C}/Γ_{7C}
$\Gamma^l_{2'}$	Γ^-_2	Γ_1	Γ^-_7	Γ_6
$\Gamma^l_{25'}$	Γ^+_5	Γ_5	Γ^+_8/Γ^+_7	Γ_8/Γ_7
Γ^l_1	Γ^+_1	Γ_{1v}	Γ^+_6	Γ_{6v}

Let us now consider the effect of spin-orbit interaction on these states. They can be divided in three types associated with the symmetry of the wave functions: the Γ_1 levels (using the T_d group notations)[15] are associated to *s*-like atomic functions and spin-orbit interaction transforms them in two degenerate levels $S\uparrow$ and $S\downarrow$ of Γ_6 symmetry. The spin-orbit interaction introduces no more splitting for these states. The Γ_3 level[15] are *d*-like atomic functions which have the symmetry of $D_1=3z^2-r^2$ and $D_2=\sqrt{3}(x^2-y^2)$. Spin-orbit interaction does not introduce splitting and the following states are

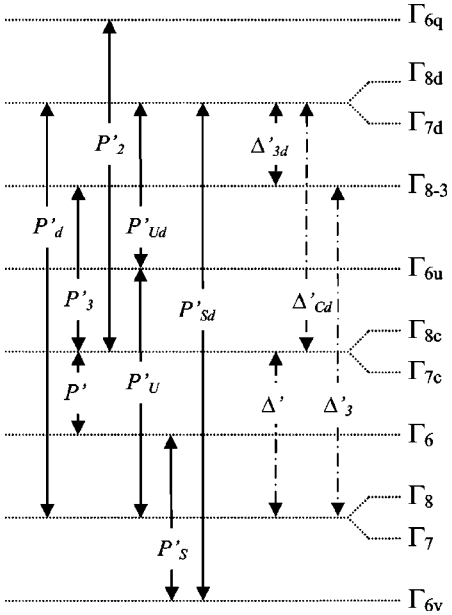

FIG. 2. T_d group: Additional matrix elements and spin-orbit coupling due to the lack of symmetry in T_d group. For the simulation of GaAs, all these elements are taken null except P' and Δ'. Δ'_j are interband spin-orbit couplings.

obtained: $D_1\uparrow$, $D_2\uparrow$, $D_1\downarrow$ and $D_2\downarrow$. The Γ_5 levels are associated to p-like functions: they are split into two levels (Γ_7,Γ_8); the Bloch functions which diagonalize the spin-orbit interaction within the multiplet (Γ_7,Γ_8) are detailed in Ref. 11. These Bloch functions do not diagonalize exactly H_{so} [Eq. (2)]: coupling terms appear between the different Γ_5 levels or between Γ_5 and Γ_3 levels.

For O_h group semiconductors (Si and Ge), splitting introduced in the Γ_5 levels by spin-orbit interaction exists

$$\Delta_{so} = \frac{3\hbar}{4m_0^2c^2}\left\langle X \left| \frac{\partial V}{\partial x}p_y - \frac{\partial V}{\partial y}p_x \right| iY \right\rangle,$$

$$\Delta_C = \frac{3\hbar}{4m_0^2c^2}\left\langle X_C \left| \frac{\partial V}{\partial x}p_y - \frac{\partial V}{\partial y}p_x \right| iY_C \right\rangle,$$

$$\Delta_d = \frac{3\hbar}{4m_0^2c^2}\left\langle X_d \left| \frac{\partial V}{\partial x}p_y - \frac{\partial V}{\partial y}p_x \right| iY_d \right\rangle.$$

Δ_{so} is a well-known value,[16] but a splitting also exists in Γ_{5C} (Δ_C) and Γ_{5d} (Δ_d) bands as shown in Fig. 1. A coupling between the two different multiplets (Γ_7,Γ_8) and $(\Gamma_{7d},\Gamma_{8d})$ also exists

$$\Delta_{dso} = \frac{3\hbar}{4m_0^2c^2}\left\langle X_d \left| \frac{\partial V}{\partial x}p_y - \frac{\partial V}{\partial y}p_x \right| iY \right\rangle.$$

There is also a coupling between $(\Gamma_{7C},\Gamma_{8C})$ multiplet which stem from Γ_{5C} levels and Γ_8 level which stem from Γ_3:

$$\Delta_{3C} = \frac{3\hbar}{4m_0^2c^2}\left\langle D_1 \left| \frac{\partial V}{\partial y}p_z - \frac{\partial V}{\partial z}p_y \right| iX_C \right\rangle.$$

For T_d group semiconductors, the inversion asymmetry of the zinc-blende lattice introduces additional spin-orbit coupling terms between the different (Γ_7,Γ_8) multiplets[11] as shown in Fig. 2. These couplings have the same expression as inside (Γ_7,Γ_8) multiplets

$$\Delta' = \frac{3\hbar}{4m_0^2c^2}\left\langle X_C \left| \frac{\partial V}{\partial x}p_y - \frac{\partial V}{\partial y}p_x \right| iY \right\rangle,$$

$$\Delta'_{Cd} = \frac{3\hbar}{4m_0^2c^2}\left\langle X_d \left| \frac{\partial V}{\partial x}p_y - \frac{\partial V}{\partial y}p_x \right| iY_C \right\rangle.$$

There are also new couplings between (Γ_7,Γ_8) multiplets which stem from Γ_5 levels and Γ_8 level which stem from Γ_3:

$$\Delta'_3 = \frac{3\hbar}{4m_0^2c^2}\left\langle D_1 \left| \frac{\partial V}{\partial y}p_z - \frac{\partial V}{\partial z}p_y \right| iX \right\rangle,$$

$$\Delta'_{3d} = \frac{3\hbar}{4m_0^2c^2}\left\langle D_1 \left| \frac{\partial V}{\partial y}p_z - \frac{\partial V}{\partial z}p_y \right| iX_d \right\rangle.$$

Figure 2 represents all the T_d couplings Δ' which are null in O_h because of inversion symmetry.

One of the interests of this method is that the matrix elements are enough to describe Luttinger parameters and Γ effective mass of conduction band. The following formulas give Luttinger parameters:

TABLE II. $k=0$ energy level used in the 30-band $\mathbf{k}\cdot\mathbf{p}$ model.

eV	Ge	Si	GaAs	eV	Ge	Si	GaAs
Γ_{8C}	3.22	3.40	4.569	Γ_{6q}	18.36	13.46	13.64
Γ_{7C}	3.01	3.40	4.488	Γ_{8d}	17.0	12.78	11.89
Γ_6	0.90	4.185	1.519	Γ_{7d}	17.0	12.78	11.89
Γ_8	0	0	0	Γ_{8-3}	10.47	9.66	10.17
Γ_7	−0.290	−0.044	−0.341	Γ_{6u}	7.77	7.07	8.56
Γ_{6v}	−13.14	−12.92	−12.55				

$$\gamma_1 = -1 + \frac{E_P}{3E_G} + \frac{E_{PX}}{3}\left(\frac{1}{E_G+E_{GC}} + \frac{1}{E_G+E_{GC}+\Delta_C}\right) + \frac{2E'_{Pd}}{3E_{5d}} + \frac{4}{3}\frac{E_{P3}}{E_3} + \frac{E_{P2}}{3E_{6q}} - \frac{E'_{PS}}{3E_{6v}} + \frac{E'_{PU}}{3E_{6u}},$$

$$\gamma_2 = \frac{1}{6}\left(\frac{E_P}{E_G} + \frac{E_{P2}}{E_{6q}} + \frac{E'_{PU}}{E_{6u}} - \frac{E'_{PS}}{3E_{6v}}\right) - \frac{E_{PX}}{6(E_G+E_{GC})} - \frac{E'_{Pd}}{6E_{5d}} + \frac{2}{3}\frac{E_{P3}}{E_{3d}},$$

$$\gamma_3 = \frac{1}{6}\left(\frac{E_P}{E_G} + \frac{E_{P2}}{E_{6q}} + \frac{E'_{PU}}{E_{6u}} - \frac{E'_{PS}}{3E_{6v}}\right) + \frac{E_{PX}}{6(E_G+E_{GC})} + \frac{E'_{Pd}}{6E_{5d}} - \frac{1}{3}\frac{E_{P3}}{E_{3d}}.$$

γ_C is also given by the matrix elements

$$\gamma_C = \frac{m_0}{m_C} = 1 + \frac{E_P}{3}\left(\frac{1}{E_G+\Delta} + \frac{2}{E_G}\right) - \frac{E'_P}{3}\left(\frac{1}{E_{GC}} + \frac{2}{E_{GC}+\Delta_C}\right) - \frac{E_{Pd}}{E_{5d}-E_G}.$$

No pseudo-Luttinger parameter is necessary to obtain valence band masses in all the directions, contrary to the 20-

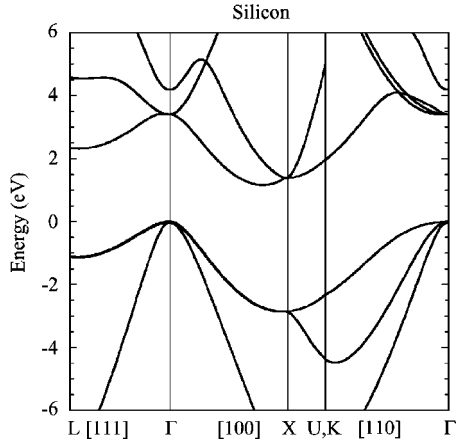

FIG. 3. Band diagram of bulk Si at $T=0$ K. Spin-orbit coupling is taken into account even if it does not appear on the diagram because of its scale. $\Delta_{so}=44$ meV in Si.

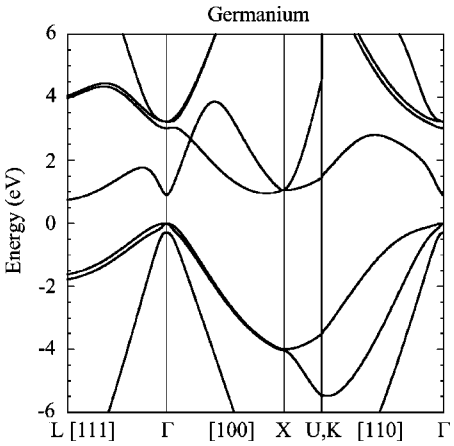

FIG. 4. Band diagram of Ge at $T=0$ K.

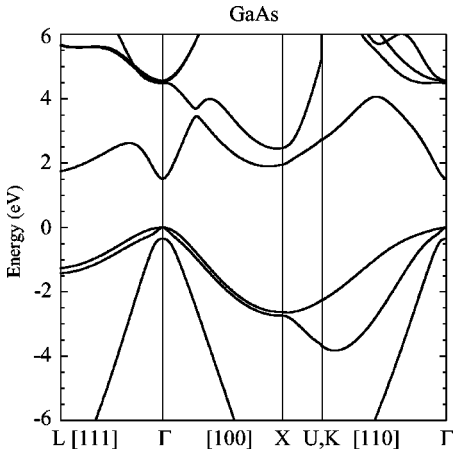

FIG. 5. Band diagram of GaAs at $T=0$ K.

band $\mathbf{k}\cdot\mathbf{p}$ Hamiltonian.[12] This 20-band Hamiltonian was built from the 14×14 Hamiltonian,[17] adding an *s*-symmetry band 12 eV under the top of the valence band and two s^* levels to obtain nonmonotonic bands and give access to *X*, Δ, or *L* valleys in the first conduction band. As these s^* levels were not sufficient to describe simultaneously the *L* point and the Γ effective masses, the contribution of *d* levels was mimicked via Luttinger-like parameters which played a part in the Γ_{7C} and Γ_{8C} levels and in the Γ_{7V} and Γ_{8V} levels by second-order perturbations. It explains why Luttinger parameters could not be obtained directly from the matrix elements, contrary to the $\mathbf{k}\cdot\mathbf{p}$ 30-band method.

Taking into account strain can be made as in Ref. 18. The same strain Hamiltonian with five parameters has to be added to the 30×30 Hamiltonian used for bulk semiconductors.

III. BAND DIAGRAMS OF Si, Ge, AND GaAs

After having built the 30×30 Hamiltonian, we now give the parameters used in our $\mathbf{k}\cdot\mathbf{p}$ calculation and describe the results for Si, Ge, and GaAs. The $k=0$ energies are presented in Table II. The left part of this table is known;[16] for the right part of Table II, we take the same values as in Ref. 5 for Si and Ge. For GaAs, these levels are unknown but Cardona and Pollak[5] explain how to obtain an estimation of these energies, knowing the form factors used in pseudopotential calculations[19] and assuming that only the pseudopotential interaction between the 30 plane-waves states is important. Anyway, the $k=0$ upper energy levels chosen are not key parameter by themselves: the important data are the couples energy level/matrix element. Briefly speaking, the $k=0$ energy levels are first fixed from Ref. 5 and the matrix elements are then adjusted to obtain the band diagram; as a result there are 10 (18) adjustable parameters in $O_h(T_d)$.

After having chosen the unknown $k=0$ energy levels, the key parameters are the matrix elements. Here, they were first estimated at the center of the Brillouin zone, especially for the valence band to obtain Luttinger parameters, and for the first conduction band for Ge and GaAs, then at the extrema *X* and *L* and finally to respect the continuity between $U\left[1,\frac{1}{4},\frac{1}{4}\right]$ and $K\left[0,\frac{3}{4},\frac{3}{4}\right]$ equivalent points of the Brillouin zone. This continuity is not obtained by construction as in pseudopotential or LCAO: on the contrary, it is the strongest numerical difficulty of this method. Figures 3–5 show the band structures of Si, Ge, and GaAs obtained with our $\mathbf{k}\cdot\mathbf{p}$ model. Numerical results are given in Table III. The band structure is well reproduced on a width of about 11 eV: it describes correctly the valence band over a 6 eV scale (see Fig. 6) and the lowest four conduction bands over a 4 eV scale in four directions namely Γ*X*, Γ*L*, Γ*K*, *XU*. All the spin-orbit parameters were taken null except Δ_{so} and Δ_C.[16]

The 30-band method represents a great improvement of the $\mathbf{k}\cdot\mathbf{p}$ method compared to the 20-band Hamiltonian whose extension was only 1 eV for the valence band and 3 eV for the conduction band.[12] This 20-band method was built to take into account the *d* level effects without directly considering this level in the Hamiltonian. The present calculation shows that taking into account the real *d* levels with their

TABLE III. Matrix elements of the momentum *p*: energies $E_{Pj}^{(\prime)}$ and matrix elements $P_j^{(\prime)}$ are linked by $E_{Pj}^{(\prime)}=(2m_0/\hbar^2)[P_j^{(\prime)}]^2$. $P_j^{(\prime)}$ are defined in the text (Sec. III) and in Figs. 2 and 3.

eV	Ge	Si	GaAs	eV	Ge	Si	GaAs
E_p	24.60	19.96	22.37	E_{Pd}	0.0051	1.193	0.010
E_{PX}	17.65	14.81	16.79	E_{PXd}	12.23	7.491	4.344
E_{P3}	5.212	4.475	4.916	E_{P3d}	15.76	9.856	8.888
E_{P2}	2.510	3.993	6.280	E_{P2d}	27.59	20.76	23.15
E_{PS}	1.071	1.092	2.434	E_{PU}	17.84	16.36	19.63
E'_P			0.0656	$E'_{Pd},E'_{P3},E'_{P2},E'_{PS},E'_{PU},E'_{PSd},E'_{PUd}$			0

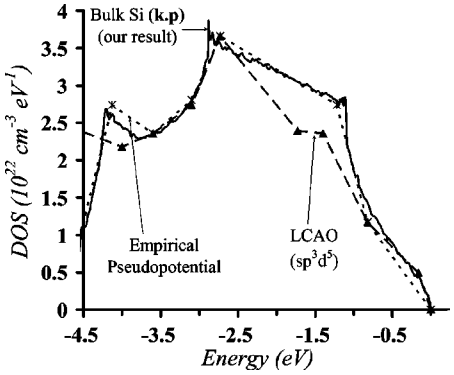

FIG. 6. Density of states in the valence band for Si. This density of states is compared to empirical pseudopotential (Ref. 19) and sp^3d^5 tight binding (Ref. 23) methods.

special symmetry, especially for D_1 and D_2 functions, makes unnecessary the pseudo-Luttinger parameters. Second-order perturbation used in 20-band $\mathbf{k}\cdot\mathbf{p}$ Hamiltonian gave access to a very good description of the center of the Brillouin zone but the effect of *d* levels on the edge of the Brillouin zone were not accounted for whereas taking into account the real *d* levels not only gives us an accurate description of the center of the Brillouin zone but also gives access to the *L* valley of second conduction band, valleys which have to be considered for accurate high energy transport simulations including impact ionization for example.[20]

In the case of GaAs, only 11 parameters were enough to obtain this band diagram. Of course, all the 18 matrix elements are adjustable terms but an accurate GaAs band diagram was obtained with only 11 nonzero matrix elements detailed in Table III. The only nonzero parameter due to the lack of inversion symmetry is P', whose value is controversial: $E'_P=(2m_0/\hbar^2)P'^2=65$ meV, far too small compared to 2.36 eV[11] or 6 or 11 eV.[21] E'_P determines the energy splitting E_{1-2} between the first and the second conduction band in zinc-blende structure ($E'_P=0$ in diamond structure). In GaAs, this splitting is equal to 0.2 eV[22] at the relevant wave vector $k=0.34$ Å^{-1} in [100] direction. E_{1-2} is equal to $2\sqrt{E'_P(\hbar^2k^2/2m_0)}$ as far as the only matrix element P' has to be considered. If we successively take $E'_P=11,6,2.36$ eV, we get $E_{1-2}=4.4,3.3,2$ eV, respectively. Whatever the E'_P value, E_{1-2} is far too large. $E_{1-2}=0.3$ eV leads to $E'_P=0.051$ eV. The complete numerical calculation taking into account all the bands leads to the value $E'_P=0.065$ eV and eventually gives a splitting of $E_{1-2}=0.23$ eV which is quite reasonable. All the bands reach the edge of the Brillouin zone with zero slope or average zero slope, as required by crystal symmetry.

The valence band is very precisely described: Table IV compares the Luttinger parameters obtained with our $\mathbf{k}\cdot\mathbf{p}$ method to the well-known values from Ref. 16. The agreement between experimental and calculated Luttinger parameters is of the order of 10% in the worst case (γ_2 of Si). Furthermore, it does not affect the density of states in valence band, which is in very good agreement with pseudopotential calculation[19] as shown in Fig. 6, and sp^3d^5 tight-binding calculation.[23] Figure 7 shows that the Si valence band diagram calculated by our $\mathbf{k}\cdot\mathbf{p}$ model is in good agreement with the pseudopotential and tight-binding methods.

TABLE IV. Effective masses in the CB and Luttinger parameters obtained with the 30-band $\mathbf{k}\cdot\mathbf{p}$ method, compared to experimental data (Ref. 16).

	γ_1	γ_2	γ_3	$m(\Gamma)$	$m_t(X)$	$m_l(X)$	$m_t(L)$	$m_l(L)$
Si ($\mathbf{k}\cdot\mathbf{p}$)	4.21	0.427	1.42		0.1912	0.9167	1.65	0.128
Si (exp)	4.26	0.38	1.56		0.1905	0.9163		
Ge ($\mathbf{k}\cdot\mathbf{p}$)	12.60	3.93	5.39	0.0380	0.195	0.93	0.818	1.593
Ge (exp)	13.35	4.25	5.69	0.038			0.815	1.59
GaAs ($\mathbf{k}\cdot\mathbf{p}$)	7.18	2.23	2.99	0.0676	0.23	1.16	0.108	1.67
GaAs (exp)	6.85	2.1	2.9	0.067	0.23	1.3	0.075	1.9

The conduction band is also described with a very good accuracy, as shown by the comparison between energy levels obtained in tight-binding,[3] experimentally,[16] and in $\mathbf{k}\cdot\mathbf{p}$ calculation (our method) presented in Table V. Even effective masses, shown in Table IV, are in very good agreement with experience: the masses of the lowest valley (Δ for Si, *L* for Ge, and Γ for GaAs) obtained with our method differ with less than 1% from experimental data. The worst case concerns transverse mass of *L* valley of GaAs, which is still nearer from the experimental value than the one obtained by Jancu *et al.*[3] in TB ($0.117\ m_0$) but except this mass, all the other differ from the experimental value with less than 10%.

The second conduction band in the ΓK direction results from the free electron dispersion $(2\pi/a)[2-x,2-x,0]$ $(0<x<3/4)$ which stems from the $(2\pi/a)[220]$ Γ point whose energy is of the order of 20 eV above the bottom of the first conduction band; bands which stem from this point were not taken into account in our $\mathbf{k}\cdot\mathbf{p}$ model as in Ref. 5. That is why continuity is not assured for the second conduction band between *K* and *U* points but this discontinuity is more than 4 eV above the bottom of the conduction band, i.e., out of the scope of our model.

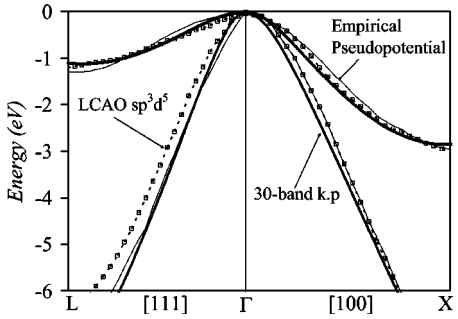

FIG. 7. Comparison of Si valence band obtained by Empirical Pseudopotential (Ref. 19), sp^3d^5 tight binding (Ref. 23), and 30-band $\mathbf{k}\cdot\mathbf{p}$ methods.

TABLE V. Comparison of energies obtained in the present work ($\mathbf{k}\cdot\mathbf{p}$) with the sp^3d^5 tight binding calculation (TB) and experimental values (exp). The TB results are taken from Ref. 3 and the experimental data from Ref. 16. Energies are in electron-volts, with the origin at the top of the valence band.

	Si			Ge				GaAs		
	$\mathbf{k}\cdot\mathbf{p}$	TB	exp	$\mathbf{k}\cdot\mathbf{p}$	TB	exp		$\mathbf{k}\cdot\mathbf{p}$	TB	exp
X_{5C}	1.36	1.35		1.04	1.12	1.30	X_{7C}	2.46	2.328	2.35
$\Delta_{\min}$	1.17	1.17	1.17	0.95	1.00		X_{6C}	1.94	1.989	1.98
X_{5V}	−2.90	−3.15	−2.90	−3.99	−3.37	−3.15	X_{7V}	−2.62	−2.929	−2.80
							X_{6V}	−2.74	−3.109	−2.88
L_{8C}	4.50	4.39	4.15	4.01	3.99	4.30	L_{8C}	5.65	5.047	5.70
L_{6C}	2.35	2.14	2.40	0.74	0.74	0.74	L_{6C}	1.75	1.837	1.85
L_{8V}	−1.10	−1.08	−1.2	−1.62	−1.12	−1.40	L_{8V}	−1.25	−1.084	−1.20
L_{7V}	−1.12	−1.12	−1.2	−1.77	−1.37	−1.40	L_{7V}	−1.42	−1.330	−1.42

Before concluding we briefly discuss the results of Ref. 13, where the band structure of GaAs is obtained over an energy range between about 15 eV below and 10 eV above the top of the valence band Γ_{8v}. As quoted in Ref. 5, the continuity of the lowest valence band (Γ_{6v}) at equivalent points of the Brillouin zone is difficult to obtain. As the Γ_{6v} band is more than 10 eV below Γ_{8v} and therefore not very useful to account for transport properties, we have chosen not to achieve the best continuity for Γ_{6v} but instead to improve the continuity of the other bands. This explains that the range of our figures is not larger than 6 eV below Γ_{8v}. This also explains why the continuity at X and U,K points for the highest valence band and the lowest conduction band is better in the figures of the present paper than in Ref. 13.

IV. CONCLUSION

The 30 band $\mathbf{k}\cdot\mathbf{p}$ model allows one to obtain a very precise description of the band diagram on the whole Brillouin zone with only 10 (for O_h group) or 11 (for T_d group) adjustable parameters. Its accuracy is comparable to the pseudopotential method with the advantages of a $\mathbf{k}\cdot\mathbf{p}$ method, i.e., a rapid access to the valence band via an explicit expression of the Luttinger parameters and an easy way to take into account strain. Compared to the 20-band $\mathbf{k}\cdot\mathbf{p}$ method, this article shows that it is easier and more efficient to take into account real d states than to mimic them by pseudo-Luttinger parameters and s^* fictive bands. This 30-band model gives access to the second conduction band: it allows one to make accurate full band transport calculation including impact ionization or other high field effects.

ACKNOWLEDGMENT

The authors thank Philippe Boucaud for a careful reading of the manuscript.

[1] L.W. Wang and A. Zunger, Phys. Rev. B **54**, 11417 (1996).
[2] M. Willatzen, M. Cardona, and N.E. Christensen, Phys. Rev. B **50**, 18054 (1994).
[3] J.M. Jancu, R. Scholz, F. Beltram, and F. Bassani, Phys. Rev. B **57**, 6493 (1998).
[4] P. Vogl, J. Hjalmarson, and J.D. Dow, J. Phys. Chem. Solids **44**, 365 (1983).
[5] M. Cardona and F. Pollak, Phys. Rev. **142**, 530 (1966).
[6] G. Dresselhaus, Phys. Rev. **100**, 580 (1955).
[7] J.M. Luttinger and W. Kohn, Phys. Rev. **97**, 869 (1955).
[8] G. Dresselhaus, A.F. Kip, and C. Kittel, Phys. Rev. **98**, 368 (1955).
[9] E.O. Kane, J. Phys. Chem. Solids **4**, 249 (1957).
[10] C.R. Pidgeon and R.N. Brown, Phys. Rev. **146**, 575 (1966).
[11] P. Pfeffer and W. Zawadzki, Phys. Rev. B **41**, 1561 (1990).
[12] N. Cavassilas, F. Aniel, K. Boujdaria, and G. Fishman, Phys. Rev. B **64**, 115207 (2001).
[13] D.W. Bailey, C.J. Stanton, and K. Hess, Phys. Rev. B **42**, 3423 (1990), and references therein.
[14] M. Cardona, N.E. Christensen, and G. Fasol, Phys. Rev. B **38**, 1806 (1988).
[15] G.F. Koster, J.O. Dimmock, R.G. Wheeler, and H. Statz, *Properties of the Thirty-Two Point Groups* (MIT Press, Cambridge, MA, 1963).
[16] *Semiconductors: Intrinsic Properties of Group IV Elements and III-V, II-VI and I-VII Compounds*, Landolt-Börnstein New Series Group III, edited by O. Madelung (Springer, Berlin, 1987), Vol. 22, Part a.
[17] P. Pfeffer and W. Zawadzki, Phys. Rev. B **53**, 12813 (1996).
[18] S. Richard, N. Cavassilas, F. Aniel, and G. Fishman, J. Appl. Phys. **94**, 1795 (2003).
[19] R.L. Chelikowsky and M.L. Cohen, Phys. Rev. B **14**, 556 (1976).
[20] N. Cavassilas, F. Aniel, G. Fishman, and R. Adde, Solid-State Electron. **46**, 559 (2002).
[21] C. Hermann and C. Weisbuch, in *Optical Orientation*, edited by F. Peir and B. P. Zakharchenya (Elsevier, British Vancouver, 1984), pp. 463–508.
[22] M.V. Fischetti and S.E. Laux, Phys. Rev. B **38**, 9721 (1988).
[23] S.Y. Ren, X. Chen, and J.D. Dow, J. Phys. Chem. Solids **59**, 403 (1998).